

Independent Estimation of Black Hole Mass for the γ -ray Detected Archetypal Narrow-Line Seyfert 1 Galaxy 1H 0323+342 from X-ray Variability

Hai-Wu Pan^{1,2}, Weimin Yuan^{1,2}, Su Yao^{3,4}, S. Komossa⁵ & Chichuan Jin¹

ABSTRACT

γ -ray detected narrow-line Seyfert 1 galaxies (NLS1s) are a newly discovered class of radio-loud active galactic nuclei (AGNs) that launch powerful jets which are generally found only in blazars and radio galaxies. However, their black hole (BH) masses as estimated from their broad emission lines are an order of magnitude or more lower than those in blazars. This poses new challenges in explaining the triggering of radio loudness in AGNs. It is still under debate whether their BH masses are underestimated by the commonly used virial method. Here we present an estimate of the BH mass for the γ -ray detected NLS1 1H 0323+342, an archetype of this class, from its X-ray variability, which is independent of inclination. Our results independently confirm that this γ -ray detected NLS1 harbors a $(2.8 - 7.9) \times 10^6 M_{\odot}$ BH similar to those in normal NLS1s rather than those in blazars.

Subject headings: galaxies: active — galaxies: nuclei — X-rays: galaxies

1. INTRODUCTION

Narrow-line Seyfert 1 galaxies (NLS1s), which are defined as active galactic nuclei (AGNs) with broad Balmer lines narrower than 2000 km s^{-1} (Osterbrock & Pogge 1985), appear mostly to be radio-quiet with radio loudness¹ $R < 10$. Only a small subset have been noticed to be radio-loud sources (e.g., Zhou et al. 2006; Komossa et al. 2006). Yuan et al. (2008) found there exists a population of genuine radio-loud NLS1s showing observational properties characteristic of blazars

with relativistic jets. The finding was confirmed and highlighted by the detection of γ -ray emission from a small number of NLS1s with the Fermi satellite (e.g., Abdo et al. 2009a,b; D’Ammando et al. 2012; Yao et al. 2015a). Radio-loud NLS1s exhibit some distinct properties compared to those classical radio-loud AGNs, e.g., blazars. Nearby NLS1s generally reside in pseudo-bulges (Mathur et al. 2012), while the common hosts of classical radio-loud AGNs are elliptical galaxies (e.g., León-Tavares et al. 2011). The key difference is the mass of the central black hole (BH).

NLS1s are thought to have lower BH masses than classical blazars and Seyfert galaxies, and hence higher Eddington ratios (see Komossa 2008; Yuan et al. 2008 for a review). However, this assertion is still under active debate at the forefront of research today. There have been studies suggesting that the BH masses of NLS1s may possibly be underestimated by the commonly used virial method involving broad optical emission lines because of the inclination effect, if their broad line regions (BLRs) are planar and seen face on (Collin & Kawaguchi 2004; Jarvis & McLure

¹Key Laboratory of Space Astronomy and Technology, National Astronomical Observatories, Chinese Academy of Sciences, 20A Datun Road, Chaoyang District, Beijing, China; panhaiwu@nao.cas.cn, wmy@nao.cas.cn

²University of Chinese Academy of Sciences, School of Astronomy and Space Science, Beijing 100049, China

³Kavli Institute for Astronomy and Astrophysics, Peking University, Beijing 100871, China

⁴National Astronomical Observatories, Chinese Academy of Sciences, Beijing, China

⁵Max-Planck Institut für Radioastronomie, Auf dem Hügel 69, 53121 Bonn, Germany

¹The radio loudness R is defined as the ratio of the radio 5 GHz flux to the optical B-band flux.

2006). Early studies have found a positive correlation between the radio loudness and BH mass in AGNs (Laor 2000). This indicates that a threshold BH mass is required for AGNs that launch powerful relativistic jets. Thus, radio-loud NLS1s have also been suggested in some studies to have supermassive BHs similar to those in blazars (e.g., Calderone et al. 2013; León Tavares et al. 2014; Baldi et al. 2016; D’Ammando et al. 2017, 2018). Moreover, observationally, NLS1s are found to be located at one extreme end in the so-called eigenvector 1 parameter space (Boroson 2002; Sulentic et al. 2008), as revealed by a set of correlations presumably driven primarily by the Eddington ratio (e.g., Boroson 2002; Grupe et al. 2010; Xu et al. 2012). These include the strong permitted Fe emission lines (Boroson & Green 1992), steep soft X-ray spectra (Wang et al. 1996) and rapid X-ray variability (Leighly 1999), etc. In contrast, most blazars lie at the other end of the eigenvector 1 parameter space (Boroson 2002). Thus, NLS1s were once thought to be radio-quiet, which turns out to be a consequence of their low radio-loud fraction (Zhou et al. 2006; Komossa et al. 2006). Thus the detection of γ -ray emitting NLS1s poses a new challenge in explaining the radio loudness in AGNs. There are other lines of evidence hinting that radio-loud NLS1s have lower BH masses than blazars, and hence higher Eddington ratios (Komossa et al. 2006; Yuan et al. 2008; Yao et al. 2015b). Therefore, an inclination-independent estimator is essential for resolving the controversy over the BH masses of NLS1s that launch relativistic jets.

Only a handful of NLS1s have been detected in γ -rays so far (Abdo et al. 2009a,b; Foschini 2011; D’Ammando et al. 2012, 2015; Yao et al. 2015a; Paliya et al. 2018; Yang et al. 2018). 1H 0323+342 is the nearest of them (redshift $z = 0.0629$), allowing detailed observational studies, e.g., of its host morphology (Zhou et al. 2007; León Tavares et al. 2014), the variability of multiwavelength emission (e.g., Paliya et al. 2014; Yao et al. 2015b), and jet structure on the scale of parsecs (Fuhrmann et al. 2016). The method of single-epoch spectra using several broad emission lines has been employed, resulting in a relatively low mass of about $\sim 2 \times 10^7 M_{\odot}$ (Zhou et al. 2007; Landt et al. 2017), and an Eddington ratio of about 0.5 – 1.0 (Landt et al. 2017). Recently, Wang et al. (2016)

used the reverberation mapping method and obtained a similar result. However, a BH mass of the order of magnitude of $10^8 M_{\odot}$ has also been suggested, based on relation between bulge luminosity and BH mass (León Tavares et al. 2014). This discrepancy can be explained in two ways: either 1H 0323+342 (and perhaps other radio-loud NLS1s too) resides in a luminous bulge (often a pseudo-bulge) that harbors a much less massive BH than what is normally predicted from the bulge luminosity, or the BH mass is underestimated by the virial method using the broad lines as a result of the inclination effect.

In this paper, we estimate the BH mass of 1H 0323+342 from the variability properties of its X-ray emission. Rapid X-ray variability is one of the basic observational characteristics of AGNs (McHardy 1985). Since the X-ray emission is thought to originate from the innermost region of an accretion flow around the BH, its variability provides a powerful tool to study the dynamics of matter very close to the BH, which is likely encoded with some of the BH parameters. In fact, some of the characteristics of X-ray variability have been used to estimate the BH mass of AGNs, including the break frequency of the power spectral density (PSD) (McHardy et al. 2006; González-Martín & Vaughan 2012), the normalized excess variance (Zhou et al. 2010; Ponti et al. 2012), and the quasi-periodic oscillation frequency (Pasham et al. 2014; Zhou et al. 2015; Pan et al. 2016). Unlike the commonly used virial method involving the line-of-sight velocities of the orbiting gas, which is susceptible to the orientation effect of AGNs (Collin & Kawaguchi 2004), X-ray variability can be considered as essentially independent of inclination. In this work, we perform X-ray timing analysis using data from a high quality X-ray observation made with the *XMM-Newton*, based on which the BH mass of 1H 0323+342 is derived from the break frequency of the PSD and the excess variance.

2. OBSERVATION AND DATA REDUCTION

1H 0323+342 was observed with *XMM-Newton* with an exposure of ~ 80 ks on 2015 August 24 in the large window imaging mode (ObsID: 0764670101). To improve the signal-to-noise ratio, the

data taken from the EPIC PN and MOS cameras are utilized. We follow the standard procedure to reduce the data and extract science products from the observation data files (ODFs) using the *XMM-Newton* Science Analysis System (version 15.0.0). Only good events (single and double pixel events, i.e., PATTERN ≤ 4 for PN or ≤ 12 for MOS) are used. Source events are extracted from a circular region of 40 arcsec radius, and background events from a source-free circle with the same radius on the same CCD chip. No pile-up effect is found for each of the detectors, by applying the EPATPLOT task. X-ray light curves are constructed for all the three EPIC cameras in the 0.2-10 keV energy band with a binsize of 10s. Final source light curves are obtained by subtracting corresponding background light curves extracted from the background regions, and corrected for instrumental factors using EPICLCCORR.

Count rate light curves of a source measured simultaneously by independent detectors can be co-added in order to increase the signal-to-noise ratio, provided that the detectors have the same responses (effective areas) or the source's spectral shape does not vary with time during the observation. Since the two MOS detectors are essentially identical and have very similar responses, the two MOS light curves are co-added into a combined MOS light curve. Figure 1 shows the PN and the combined MOS light curves. Although the PN and MOS detectors have different responses, the two light curves follow each other closely, indicating weak or no changes in the spectral shape. This can be demonstrated by the ratio of the two light curves (bottom panel in Figure 1), which appears to be constant. We thus also co-added the PN and MOS light curves ($CR_{\text{total}}=CR_{\text{PN}}+CR_{\text{MOS1}}+CR_{\text{MOS2}}$) to form a combined single PN+MOS light curve of the source, assuming no significant spectral variations during the observation. The combined light curve for all the detectors is shown in Figure 2. In the following analysis, both the PN and MOS light curves are used individually, as well as the combined single source light curve with the best signal-to-noise ratio for comparison. As shown in Figure 1 and Figure 2, the X-ray emission of 1H 0323+342 exhibits significant variability on various timescales, typical of NLS1 galaxies.

During the whole observation the particle back-

ground is at a normal level except for the last ~ 15 ks when an enhanced background flare occurred. We have carefully inspected the data set for a possible influence of the background on the measured light curves, and especially during the intervals of the flaring background. We find that the background is significantly fainter (mean count rate=0.05 counts s $^{-1}$; Figure 1) than the source, which is rather bright (mean count rate=7.80 counts s $^{-1}$). Even during the period of enhanced background toward the end of the observation, the background is more than five times fainter than the source for each time bin. We therefore consider the effect of background fluctuations on the measured light curves to be negligible, and thus make use of the full, uninterrupted source light curve for timing analysis.

3. TIMING ANALYSIS AND ESTIMATION OF BH MASS

3.1. Power Spectral Density

Early studies showed that the PSD of AGNs could be described by a simple power law (Lawrence & Papadakis 1993), whereas later investigations with high quality PSDs revealed a flattening toward the low frequency end (e.g., Papadakis & McHardy 1995). It has been established that the AGN PSD can be best described by a bending (or broken) power law, with two slopes with universal values of ~ -2 in the high frequency part and ~ -1 in the low frequency part (Markowitz et al. 2003; Vaughan et al. 2003a). McHardy et al. (2006) first suggested a tight correlation between the bend/break frequency ν_b and the BH mass as well as the bolometric luminosity over a wide range of BH masses from black hole X-ray binary (BHXB) to AGN. Using a larger sample of AGNs, González-Martín & Vaughan (2012) found a similar result, but with a weaker dependence on the bolometric luminosity. This indicates that the bend/break frequency depends mostly on the BH mass.

In the analysis below, the combined PN+MOS light curve is mainly used, given its highest signal-to-noise ratio, while the PN and the combined MOS light curves are also analyzed for the purpose of comparison of results. The PSDs of the light curves of 1H 0323+342 are computed as the modulus-squared of the discrete Fourier trans-

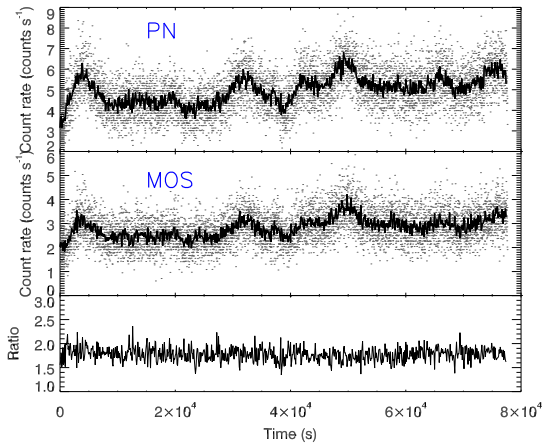


Fig. 1.— The PN (upper panel) and combined MOS (MOS1+MOS2; middle panel) light curves of 1H 0323+342 in the energy band of 0.2-10 keV. The black lines represent the light curves with a binsize of 100s, while those with a binsize of 10s are plotted in gray. The ratio between the PN and combined MOS (MOS1+MOS2) light curves is plotted in the lower panel.

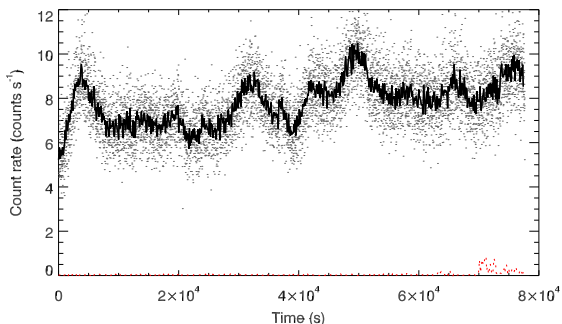


Fig. 2.— X-ray light curve of 1H 0323+342 obtained with *XMM-Newton*, which is a combination of background-subtracted light curves extracted from the PN, MOS1 and MOS2 detectors in 0.2-10 keV. The black line represents the light curve with a binsize of 100s, while the one with a binsize of 10s is plotted in gray. The background (red dashed line) is significantly fainter than the source.

form, and the $(\text{rms}/\text{mean})^2$ normalization is chosen (Vaughan et al. 2003b). The PSD derived from the combined PN+MOS light curve is shown in Figure 3. It shows a typical red-noise spectrum in the frequency range from 10^{-5} to 10^{-3} Hz, while above 10^{-3} Hz it is dominated by Poisson noise. As can be seen, a flattening toward the low frequency end is apparent in the red noise of the PSD.

We first fit the PSD with a model of a simple power-law (red noise) plus a constant (Poisson noise): $P(\nu) = N\nu^{-\alpha} + C$ (González-Martín & Vaughan 2012, see also the H_0 model in Vaughan 2010), where the normalization N , power-law index α and additive constant C are all set to be free parameters. The maximum likelihood method is used to find the best-fitting model parameters by minimizing the fit statistic S which is (twice) the minus log-likelihood (González-Martín & Vaughan 2012; see also Vaughan 2010), yielding a slope of 2.47 ± 0.18 (the red line in Figure 3). The uncertainty of each parameter can be estimated by finding the range of parameter values for which $\Delta S \leq 1.0$, corresponding to a significance level of 68.3% (Cash 1979; González-Martín & Vaughan 2012). However, a single power-law does not describe the PSD well in the low frequency regime. Judging from the data/model residuals (see the middle panel of Figure 3), the slope of the PSD appears to flatten at around a frequency of 10^{-4} Hz. Thus we adopt a bending power-law ($P(\nu) = N\nu^{-1}(1 + \{\frac{\nu}{\nu_b}\}^{\alpha-1})^{-1} + C$) (González-Martín & Vaughan 2012, see also the H_1 model in Vaughan 2010) instead of a simple power-law to fit the PSD. The low-frequency slope is fixed to be the canonical value -1 for AGNs found from long-term X-ray monitoring studies (e.g., Markowitz et al. 2003; McHardy et al. 2006), given the relatively poor data quality at the low-frequency end (González-Martín & Vaughan 2012). The high-frequency slope is fitted to be 3.66 ± 0.54 , with a bend frequency of 1.9×10^{-4} Hz. Hence, the likelihood ratio test (LRT) suggested in Vaughan (2010) (see also González-Martín & Vaughan 2012) is used to select between the simple power-law and bending power-law models, giving a posterior predictive p -value $p = 9 \times 10^{-5}$ from the Markov Chain Monte Carlo (MCMC) simulations². This indicates that the PSD for 1H 0323+342

²As outlined in Vaughan (2010), 100,000 sets of parameters

is well described by a bending power-law, as commonly found in Seyfert AGNs.

We also analyze the PSDs of the PN and combined MOS light curves. Both PSDs can be fitted better by a bending power-law better, with a p -value of $p = 3.2 \times 10^{-4}$ (PN) or $p = 2.0 \times 10^{-4}$ (MOS) based on the LRT method, respectively, as shown in the Figure 4. The fitted bend frequencies are 2.1×10^{-4} Hz (PN) and 2.3×10^{-4} Hz (MOS), respectively, which are consistent with each other as well as that obtained from the combined PN+MOS light curve. Thus, the bend frequency of 1.9×10^{-4} Hz obtained from the combined light curve is used to estimate the BH mass of 1H 0323+342 hereinafter. Besides, we also fit the PSD of 1H 0323+342 with a broken power-law model, given that the break frequency may be slightly different from the bend frequency, as discussed in Vaughan (2010). The fitted break frequency is 2.0×10^{-4} Hz, which is consistent with the bend frequency derived above.

The relation between the bend/break frequency and the BH mass as well as the bolometric luminosity was first suggested by McHardy et al. (2006). Later González-Martín & Vaughan (2012) have found that the relation depends weakly on the bolometric luminosity, thus a relation only between the bend/break frequency and the BH mass is also suggested. All these relations are considered for the BH estimations of 1H 0323+342, and the results are listed in Table 1. First, we derive the BH mass for 1H 0323+342 from the bend frequency of 1.9×10^{-4} Hz using the relation with BH mass only:

$$\log(T_b) = (1.09 \pm 0.21) \log(M_{BH}) + (-1.70 \pm 0.29), \quad (1)$$

where T_b is the bend timescale ($T_b = 1/\nu_b$)

have been simulated from the Metropolis-Hastings MCMC algorithm, based on the best-fitting (simple power-law) model parameters (and their errors). Each set of simulated parameters can be used to generate a periodogram. Then the two models (simple power-law and bending power-law) are fitted to the same simulated periodogram to obtain the LRT statistic. Here the LRT statistic is defined as the difference between twice the minimum log-likelihood of the two models. Thus we can get the posterior predictive p -value by comparing the LRT statistic for the observed data with the distribution of this statistic obtained from the simulated data. See Vaughan (2010) and the appendices therein for details.

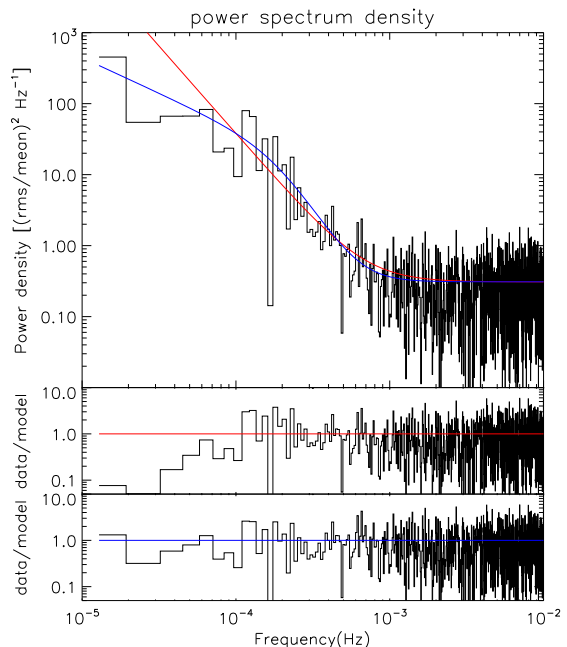


Fig. 3.— Power spectral densities of the combined PN+MOS X-ray light curve of 1H 0323+342. The red solid line represents the best-fit power-law, while the blue solid line donates the best-fit bending power-law. The data/model residuals for power-law and bending power-law models are shown in the middle and bottom panel, respectively.

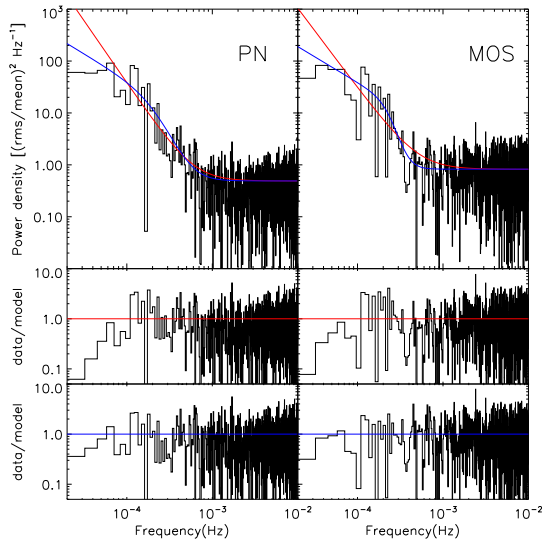


Fig. 4.— Power spectral densities of the PN and combined MOS light curves of 1H 0323+342. The red solid lines represent the best-fit power-law, while the blue solid lines donate the best-fit bending power-law. The data/model residuals for power-law and bending power-law models are shown in the middle and bottom panels, respectively.

(González-Martín & Vaughan 2012)³. The BH mass is estimated to be $2.8 \times 10^6 M_{\odot}$. The uncertainty range is calculated from Monte Carlo simulations, in which the uncertainties of the parameters in the correlations (McHardy et al. 2006; González-Martín & Vaughan 2012) as well as $\log(T)$ and $\log(M_{\text{BH}})$ are assumed to follow a Gaussian distribution.⁴ For $\log(T)$ with a value of $-1.22^{+0.15}_{-0.11}$, the uncertainty is computed via the propagation of error from the bend frequency.

Next we estimate the BH mass for 1H 0323+342 using the relation that depends on both the BH mass and bolometric luminosity. Using the bolometric correction factor (Elvis et al. 1994), Zhou et al. (2007) obtained a bolometric luminosity of $1.2 \times 10^{45} \text{ ergs s}^{-1}$ for 1H 0323+342 from its luminosity at 5100 Å. Wang et al. (2016) monitored 1H 0323+342 for more than two months using the Lijiang 2.4 m Telescope, and obtained a mean L_{5100} of $7.52 \times 10^{43} \text{ ergs s}^{-1}$. The bolometric luminosity can be estimated as $9L_{5100}$ by making use of the bolometric correction factor suggested in Kaspi et al. (2000). The value $6.77 \times 10^{44} \text{ ergs s}^{-1}$ is nearly consistent with the result in Zhou et al. (2007), indicating that the optical variability of the source is weak on a timescale of about 10 years. We make use of the relationship suggested in McHardy et al. (2006):

$$\log(T_b) = (2.17^{+0.32}_{-0.25}) \log(M_{\text{BH}}) + (-0.90^{+0.3}_{-0.2}) \log(L_{\text{bol}}) + (-2.42^{+0.22}_{-0.25}) \quad (2)$$

as well as the relationship in González-Martín & Vaughan (2012):

$$\log(T_b) = (1.34 \pm 0.36) \log(M_{\text{BH}}) + (-0.24 \pm 0.28) \log(L_{\text{bol}}) + (-1.88 \pm 0.36). \quad (3)$$

The BH mass of 1H 0323+342 is estimated to be $7.9 \times 10^6 M_{\odot}$ (Equation 2) or $4.4 \times 10^6 M_{\odot}$ (Equation 3), using the bolometric luminosity of

³ T_b is in units of days, M_{BH} in units of $10^6 M_{\odot}$, and L_{bol} in units of $10^{44} \text{ ergs s}^{-1}$ for the equations from McHardy et al. (2006) and González-Martín & Vaughan (2012).

⁴The same method is also used for the following estimations for the uncertainty of BH mass. For some parameters as well as measurements, the errors are not symmetric. In this case, the relatively larger value of error will be used. Thus the uncertainties will be a little overestimated.

$6.77 \times 10^{44} \text{ ergs s}^{-1}$ (Wang et al. 2016). The BH mass will be $1.0 \times 10^7 M_\odot$ and $4.8 \times 10^6 M_\odot$ if the bolometric luminosity of $1.2 \times 10^{45} \text{ ergs s}^{-1}$ (Zhou et al. 2007) is used, which is consistent with the former results.

Finally, we calculate the PSDs of 1H 0323+342 separately for the soft-band light curve (0.2-1.0 keV) and the hard-band light curve (2.0-10.0 keV). We find that both PSDs show similar results to those presented above for the full band, albeit with lower significance of the existence of the bend/break frequency.

3.2. Excess Variance

Besides the PSD, the normalized excess variance of X-ray variations (σ_{rms}^2) is also a useful and convenient tool to describe the variability amplitude. Following Nandra et al. (1997), the normalized excess variance can be calculated using the definition

$$\sigma_{\text{rms}}^2 = \frac{1}{N\mu^2} \sum_{i=1}^N \left[(X_i - \mu)^2 - \sigma_i^2 \right], \quad (4)$$

where N is the number of good time bins of an X-ray light curve, μ the unweighted arithmetic mean of the count rates, X_i and σ_i the count rates and their uncertainties, respectively, in each bin.

It has been shown that the tight inverse correlation between the X-ray excess variance and the BH mass of AGNs can be used to estimate the BH mass of AGNs (Lu & Yu 2001; Papadakis 2004; Zhou et al. 2010). Ponti et al. (2012) reaffirmed this relationship by making use of a large sample of 161 AGNs observed with *XMM-Newton*, and found a small scatter of 0.4 dex from the reverberation mapping sample. In fact, the $M_{\text{BH}} - \sigma_{\text{rms}}^2$ relation is actually a manifestation of the inverse scaling of the break frequency of the AGN PSD with the BH mass, since the excess variance is the integral of the PSD over the frequency domain (Papadakis 2004; Pan et al. 2015).

We calculate the excess variances on a timescale of 40 ks, using the light curve of 1H 0323+342 with a binsize of 250 s and energy of 2-10 keV from the PN camera only, which is the same as in Ponti et al. (2012). The resulting excess variance is 0.0145. A problem of this method is the large uncertainty, which comes from two sources: one is the measurement uncertainty and the other is

the stochastic nature of the variability process, which is non-negligible (Vaughan et al. 2003b; Allevato et al. 2013). The measurement uncertainty is calculated from the equation given in Vaughan et al. (2003b), while the stochastic scatter is computed from the simulation method (see Vaughan et al. 2003b; Pan et al. 2015 for more details), using the best-fit bending power-law PSD model (the Poisson noise is set to be zero) described in Section 3.1. We simulate 1000 light curves using the method of Timmer & Koenig (1995) with a binsize of 250 s and duration of 40 ks. The distribution of the calculated excess variances of all the light curves is obtained, from which the range of stochastic uncertainty at the significance level of 68% is found: $\Delta \log(\sigma_{\text{rms}}^2) = -0.25$ and $+0.16$. The total uncertainties are then obtained by combining in quadrature the stochastic and measurement uncertainties, which are at the 68% confidence level. The BH mass for 1H 0323+342 is derived using the relation suggested in Ponti et al. (2012):

$$\log(\sigma_{\text{rms}}^2) = (-2.00 \pm 0.13) + (-1.32 \pm 0.14) \log(M_{\text{BH}}/10^7 M_\odot), \quad (5)$$

yielding a BH mass of $7.5 \times 10^6 M_\odot$.

In fact, it has been suggested that the $M_{\text{BH}} - \sigma_{\text{rms}}^2$ relation flattens at $\sim 10^6 M_\odot$, below which the excess variances tend to remain constant around 0.01 (Ludlam et al. 2015; Pan et al. 2015). For 1H 0323+342, the value of excess variance is around 0.01, indicating that the BH mass is likely of the order of $\sim 10^6 M_\odot$ or even lower.

4. SUMMARY AND DISCUSSION

Thanks to the long, uninterrupted, and high quality X-ray observation with *XMM-Newton*, we are able to estimate the BH mass for the archetypal NLS1-blazar hybrid AGN 1H 0323+342 independently from the X-ray variability, which is free from the possible orientation effect of the BLR. The PSD of the light curve can be better fitted with a bending(broken) power-law model than a simple power-law, with a bend frequency of $1.9 \times 10^{-4} \text{ Hz}$. The previously established relationships between the PSD bend/break frequency and the BH mass (and possibly bolometric luminosity), as suggested by McHardy et al. (2006) and González-Martín & Vaughan (2012), are employed. The BH mass for 1H 0323+342 is con-

TABLE 1
ESTIMATED BH MASS FOR 1H 0323+342

Measurements	$\log(M_{\text{BH}}/M_{\odot})$	Reference
From the PSD bend frequency		
$f_{\text{bend}} = 1.9^{+0.66}_{-0.49} \times 10^{-4}$ Hz	6.4 ± 0.3	1
$f_{\text{bend}} = 1.9^{+0.66}_{-0.49} \times 10^{-4}$ Hz	6.6 ± 0.5	1
$L_{\text{bol}} = 6.77 \times 10^{44}$ ergs $^{-1}$		
$f_{\text{bend}} = 1.9^{+0.66}_{-0.49} \times 10^{-4}$ Hz	6.9 ± 0.2	2
$L_{\text{bol}} = 6.77 \times 10^{44}$ ergs $^{-1}$		
From the normalized excess variance of variability		
$\sigma_{\text{rms},40\text{ks}}^2 = (1.45^{+0.64}_{-0.65}) \times 10^{-2}$	6.9 ± 0.2	3

NOTE.—Column 1: the BH mass estimators with the uncertainties at the 1σ level; Column 2: BH mass derived from different methods for 1H 0323+342, with the uncertainties at the 1σ level; Column 3: corresponding references, 1-González-Martín & Vaughan (2012), 2-McHardy et al. (2006), 3-Ponti et al. (2012).

strained in the range of $(2.8 - 7.9) \times 10^6 M_{\odot}$, hence the Eddington ratio of $0.68 - 1.92$. As an alternative approach, we also calculate the normalized excess variances of the light curve, giving a BH mass consistent with the results from the PSD break. All these estimates are in reasonable agreement with one another, given the relatively large uncertainties that are calculated from Monte Carlo simulations (see Table 1).

It should be noted that the BH mass—variability relationships used in this paper are based on studies of radio-quiet AGNs. Although 1H 0323+342 is radio-loud, there is strong evidence (based on the X-ray spectral shape and multi-wavelength spectral energy distribution) that its X-ray emission below 10 keV is predominantly from the disk/corona rather than from the relativistic jets, as in radio-quiet AGNs (Yao et al. 2015b). A similar conclusion was also reached by Kynoch et al. (2018), who analyzed the same *XMM-Newton* observation used in this paper. In fact, Yao et al. (2015b) also calculated the X-ray normalized excess variance using a *Suzaku* observation with somewhat lower data quality and estimated a BH mass $\sim 8.6 \times 10^6 M_{\odot}$. The same practice using *Nustar* data was applied by Landt et al. (2017) and a similar result $\sim 1.7 \times 10^7 M_{\odot}$ was obtained. These results are consistent with our estimates from the excess variance. The BH mass derived independently from the X-ray variability for 1H 0323+342 is thus in agreement with

that of $\sim 2 \times 10^7 M_{\odot}$ estimated from the broad optical/infrared emission lines (Zhou et al. 2007; Wang et al. 2016; Landt et al. 2017), which has a typical systematics of ~ 0.3 dex.

Laor (2000) found that radio-loud AGNs tend to have BH masses larger than $3 \times 10^8 M_{\odot}$. Furthermore, Ho (2002) demonstrated that radio loudness is strongly inversely correlated with the Eddington ratio. The small BH mass and high Eddington ratio found in 1H 0323+342 are at odds with the above findings. If the BH mass found for 1H 0323+342 is typical of radio-loud NLS1s with relativistic jets, this would imply a new parameter space in which relativistic jets can also be produced, i.e., AGNs with relatively small BH masses and high Eddington ratios (see Komossa et al. 2006; Yuan et al. 2008). An interesting analogy was also suggested to BHXBs, which can also produce (transient) jets at the very high state when the Eddington ratios are the highest (e.g., Yuan et al. 2008).

Moreover, the consistency of the X-ray variability and virial estimation of the BH mass implies that the BLR in this NLS1 is not heavily flattened, because we have a near pole-on view of 1H 0323+342 as shown by Fuhrmann et al. (2016). Given that 1H 0323+342 is just an individual case, more γ -ray emitting NLS1s with long, continuous and high quality X-ray observations are further needed to provide an independent estimations of BH mass.

This work is supported by the National Natural Science Foundation of China (Grant No.11473035). S. Y. thanks the support from the KIAA-CAS fellowship. This work is based on observations obtained with *XMM-Newton*, an ESA science mission with instruments and contributions directly funded by ESA Member States and NASA. This research has made use of the NASA/IPAC Extragalactic Database (NED).

REFERENCES

- Abdo, A. A., Ackermann, M., Ajello, M., et al. 2009a, *ApJ*, 699, 976
- Abdo, A. A., Ackermann, M., Ajello, M., et al. 2009b, *ApJ*, 707, L142
- Allevato, V., Paolillo, M., Papadakis, I., & Pinto, C. 2013, *ApJ*, 771, 9
- Baldi, R. D., Capetti, A., Robinson, A., Laor, A., & Behar, E. 2016, *MNRAS*, 458, L69
- Boroson, T. A., & Green, R. F. 1992, *ApJS*, 80, 109
- Boroson, T. A. 2002, *ApJ*, 565, 78
- Calderone, G., Ghisellini, G., Colpi, M., & Dotti, M. 2013, *MNRAS*, 431, 210
- Cash, W. 1979, *ApJ*, 228, 939
- Collin, S., & Kawaguchi, T. 2004, *A&A*, 426, 797
- D’Ammando, F., Orienti, M., Finke, J., et al. 2012, *MNRAS*, 426, 317
- D’Ammando, F., Orienti, M., Larsson, J., & Giroletti, M. 2015, *MNRAS*, 452, 520
- D’Ammando, F., Acosta-Pulido, J. A., Capetti, A., et al. 2017, *MNRAS*, 469, L11
- D’Ammando, F., Acosta-Pulido, J. A., Capetti, A., et al. 2018, *MNRAS*, 478, L66
- Elvis, M., Wilkes, B. J., McDowell, J. C., et al. 1994, *ApJS*, 95, 1
- Fuhrmann, L., Karamanavis, V., Komossa, S., et al. 2016, *Research in Astronomy and Astrophysics*, 16, 176
- Foschini, L. 2011, *Narrow-Line Seyfert 1 Galaxies and their Place in the Universe*, 24
- González-Martín, O., & Vaughan, S. 2012, *A&A*, 544, A80
- Grupe, D., Komossa, S., Leighly, K. M., & Page, K. L. 2010, *ApJS*, 187, 64
- Ho, L. C. 2002, *ApJ*, 564, 120
- Jarvis, M. J., & McLure, R. J. 2006, *MNRAS*, 369, 182
- Kaspi, S., Smith, P. S., Netzer, H., et al. 2000, *ApJ*, 533, 631
- Komossa, S., Voges, W., Xu, D., et al. 2006, *AJ*, 132, 531
- Komossa, S. 2008, *Revista Mexicana de Astronomia y Astrofisica Conference Series*, 32, 86
- Kynoch, D., Landt, H., Ward, M. J., et al. 2018, *MNRAS*, 475, 404
- Landt, H., Ward, M. J., Baloković, M., et al. 2017, *MNRAS*, 464, 2565
- Lawrence, A., & Papadakis, I. 1993, *ApJ*, 414, L85
- Laor, A. 2000, *ApJ*, 543, L111
- Leighly, K. M. 1999, *ApJS*, 125, 297
- León-Tavares, J., Valtaoja, E., Chavushyan, V. H., et al. 2011, *MNRAS*, 411, 1127
- León Tavares, J., Kotilainen, J., Chavushyan, V., et al. 2014, *ApJ*, 795, 58
- Lu, Y., & Yu, Q. 2001, *MNRAS*, 324, 653
- Ludlam, R. M., Cackett, E. M., Gültekin, K., et al. 2015, *MNRAS*, 447, 2112
- Mathur, S., Fields, D., Peterson, B. M., & Grupe, D. 2012, *ApJ*, 754, 146
- Markowitz, A., Edelson, R., Vaughan, S., et al. 2003, *ApJ*, 593, 96
- McHardy, I. 1985, *Space Sci. Rev.*, 40, 559
- McHardy, I. M., Koerding, E., Knigge, C., Uttley, P., & Fender, R. P. 2006, *Nature*, 444, 730
- Nandra, K., George, I. M., Mushotzky, R. F., Turner, T. J., & Yaqoob, T. 1997, *ApJ*, 476, 70

- Osterbrock, D. E., & Pogge, R. W. 1985, *ApJ*, 297, 166
- Paliya, V. S., Sahayanathan, S., Parker, M. L., et al. 2014, *ApJ*, 789, 143
- Paliya, V. S., Ajello, M., Rakshit, S., et al. 2018, *ApJ*, 853, L2
- Pan, H.-W., Yuan, W., Zhou, X.-L., Dong, X.-B., & Liu, B. 2015, *ApJ*, 808, 163
- Pan, H.-W., Yuan, W., Yao, S., et al. 2016, *ApJ*, 819, L19
- Papadakis, I. E., & Lawrence, A. 1993, *MNRAS*, 261, 612
- Papadakis, I. E., & McHardy, I. M. 1995, *MNRAS*, 273, 923
- Papadakis, I. E. 2004, *MNRAS*, 348, 207
- Pasham, D. R., Strohmayer, T. E., & Mushotzky, R. F. 2014, *Nature*, 513, 74
- Ponti, G., Papadakis, I., Bianchi, S., et al. 2012, *A&A*, 542, A83
- Sulentic, J. W., Zamfir, S., Marziani, P., & Dultzin, D. 2008, *Revista Mexicana de Astronomia y Astrofisica Conference Series*, 32, 51
- Timmer, J., & Koenig, M. 1995, *A&A*, 300, 707
- Vaughan, S., Fabian, A. C., & Nandra, K. 2003a, *MNRAS*, 339, 1237
- Vaughan, S., Edelson, R., Warwick, R. S., & Uttley, P. 2003b, *MNRAS*, 345, 1271
- Vaughan, S. 2010, *MNRAS*, 402, 307
- Wang, T., Brinkmann, W., & Bergeron, J. 1996, *A&A*, 309, 81
- Wang, F., Du, P., Hu, C., et al. 2016, *ApJ*, 824, 149
- Xu, D., Komossa, S., Zhou, H., et al. 2012, *AJ*, 143, 83
- Yang, H., Yuan, W., Yao, S., et al. 2018, arXiv:1801.03963
- Yao, S., Yuan, W., Zhou, H., et al. 2015a, *MNRAS*, 454, L16
- Yao, S., Yuan, W., Komossa, S., et al. 2015b, *AJ*, 150, 23
- Yuan, W., Zhou, H. Y., Komossa, S., et al. 2008, *ApJ*, 685, 801-827
- Zhou, H., Wang, T., Yuan, W., et al. 2006, *ApJS*, 166, 128
- Zhou, H., Wang, T., Yuan, W., et al. 2007, *ApJ*, 658, L13
- Zhou, X.-L., Zhang, S.-N., Wang, D.-X., & Zhu, L. 2010, *ApJ*, 710, 16
- Zhou, X.-L., Yuan, W., Pan, H.-W., & Liu, Z. 2015, *ApJ*, 798, LL5